

# Kelvin Probe Force Microscopy Study of LaAlO<sub>3</sub>/SrTiO<sub>3</sub> Heterointerfaces

Vladimir N. Popok<sup>1,\*</sup>, Alexey Kalabukhov<sup>2</sup>, Robert Gunnarsson<sup>2,3</sup>,  
Sergey Lemeshko<sup>4</sup>, Tord Claeson<sup>2</sup>, and Dag Winkler<sup>2</sup>

<sup>1</sup>Department of Physics, University of Gothenburg, 41296 Gothenburg, Sweden

<sup>2</sup>Department of Microtechnology and Nanoscience - MC2,  
Chalmers University of Technology, 41296 Gothenburg, Sweden

<sup>3</sup>HLK, Jönköping University, 55111 Jönköping, Sweden

<sup>4</sup>NT-MDT Europe B.V., High Tech Campus Eindhoven, 5656 AG Eindhoven, The Netherlands

Surface potential distributions in ultra-thin (0.8–3.9 nm) LaAlO<sub>3</sub> layers deposited on SrTiO<sub>3</sub> substrates are studied. It is found that the potential distribution evolves from island-like to a homogeneous one with increasing LaAlO<sub>3</sub> thickness. It is suggested that the observed islands are caused by a locally enhanced concentration of mobile charge carriers at the interface that is, in turn, related to non-stoichiometry of the layers with thickness below 4 unit cells. Transition to a homogeneous potential distribution with increasing LAO thickness ( $\geq 4$  unit cells) corresponds to the formation of a quasi-2-dimensional electron gas. The results agree with a percolation model explaining the insulator-to-metal transition that occurs at the LaAlO<sub>3</sub>/SrTiO<sub>3</sub> heterointerface.

**Keywords:** LaAlO<sub>3</sub>/SrTiO<sub>3</sub> Heterointerface, Kelvin Probe Force Microscopy.

## 1. INTRODUCTION

Interfaces between complex oxides, in particular heterostructures with only a few unit cells (uc) thick LaAlO<sub>3</sub> (LAO) film on a single crystal SrTiO<sub>3</sub> (STO) substrate, are of increasing interest in oxide electronics due to the formation of a quasi-2-dimensional electron gas (q2DEG) that can exhibit magnetism, superconductivity and giant electric field effect.<sup>1–4</sup> A transition from an insulating to a conductive state occurs at a critical thickness of LAO of 4 uc.<sup>3</sup> However, identification of the source of charge carriers is still a challenging problem. Several mechanisms were suggested to explain the formation of the q2DEG such as a polar discontinuity at the interface,<sup>5</sup> creation of high density of oxygen vacancies in an STO layer<sup>6,7</sup> and interdiffusion of La into the substrate.<sup>8</sup> Recently, we found using medium-energy ion spectroscopy (MEIS) that LAO films with thicknesses  $< 4$  uc are non-stoichiometric.<sup>9</sup> Mutual diffusion of La into STO and Sr into LAO was suggested. Such interdiffusion was also observed by high-resolution transmission electron microscopy.<sup>10,11</sup> These data together with preliminary Kelvin probe force microscopy (KPFM) studies allowed us to propose a percolative model to

explain the insulator-to-metal transition in the LAO/STO interfaces.<sup>9</sup> In this paper, we present detailed KPFM investigations of the LAO/STO interface and explain how the observed change in the distribution of surface potential correlates with the evolution of the interface composition and the proposed percolative model.

## 2. EXPERIMENTAL DETAILS

LAO layers with thicknesses of 2–10 uc (1 uc  $\approx$  0.39 nm) were grown by pulsed laser ablation on (001)STO substrates kept at 800 °C and at oxygen pressure of  $10^{-4}$  mbar. The thickness of the layers was *in situ* controlled using reflection high energy electron diffraction. An additional *in situ* oxidation for all samples was done in 500 mbar oxygen at 600 °C for 2 hours. More details on the growth procedure can be found in Ref. [7]. The samples having 4 uc or thicker LAO layers showed electrical resistivity of about  $5 \times 10^4 \Omega/\square$  at room temperature and metallic temperature dependence of electrical resistance. The samples with thinner LAO layers were found to be insulating ( $> 10^{10} \Omega/\square$ ).

The samples were studied *ex situ* by atomic force microscopy (AFM) in a tapping mode and by KPFM using a Probe NanoLaboratory Ntegra-Aura (from NT-MDT). Commercial Si cantilevers with conductive TiN coating

\*Author to whom correspondence should be addressed.

<sup>†</sup>Present address: Institute of Physics, University of Rostock, Universitätsplatz 3, 18051 Rostock, Germany.

(curvature radius of a tip is about 35–40 nm) were utilized, providing a lateral resolution of KPFM images better than 100 nm. In order to obtain typical and reproducible images, measurements were carried out on a few samples for each LAO thickness. A two-pass technique was used to record AFM and KPFM images. During the first pass, topography image was acquired and used as a feedback signal in the second pass. For the second pass, the cantilever was lifted for  $z = 10$  nm from the surface. The cantilever was electrically excited by a voltage  $V_{\text{tip}} = V_{\text{dc}} + V_{\text{ac}} \sin(\omega t)$ , where  $V_{\text{ac}}$  is the driving voltage (typically 2 V in our case) at resonant frequency  $\omega$ . Thus, the capacitive force between the cantilever tip and a surface having its own potential  $\varphi$  can be written as

$$F_{\text{cap}} = \frac{1}{2}(V_{\text{tip}} - \varphi)^2 \frac{\partial C(z)}{\partial z} \quad (1)$$

where  $C(z)$  is the tip-surface capacitance. In KPFM, the first harmonic of the force,  $((V_{\text{dc}} - \varphi)V_{\text{ac}} \sin(\omega t))dC(z)/dz$ , is extracted and then nullified by adjusting the dc component of the voltage to be equal to the potential at every point on the surface ( $V_{\text{dc}} = \varphi$ ). This allows to map the surface potential in 2D.<sup>12, 13</sup>

For metals or semiconductors, the measurements of contact potential difference between a cantilever and a surface can give quantitative data regarding electronic structure of the surface, for instance, the local work function difference (in metals), local dopant concentration or electronic band bending (in semiconductors).<sup>13, 14</sup> In the case of dielectric surfaces, an analogy between the interaction of a point charge  $Q$  and a dielectric surface can be applied. This gives the electrostatic force<sup>15</sup>

$$F_{\text{diel}} = -\frac{1}{4\pi\epsilon_0} \left( \frac{\epsilon - 1}{\epsilon + 1} \right) \frac{Q^2}{4z^2} \quad (2)$$

Since the force depends on the dielectric constant  $\epsilon$  and the charge  $Q$ , the tip-surface interaction should be interpreted in terms of dielectric properties of the material as well as surface and interior charge density.<sup>16, 17</sup> It was found that  $\epsilon$  for LAO depends on the layer thickness.<sup>18</sup> However, one can see from Eq. (2) that, for instance, a doubling of  $\epsilon$  leads only to a small increase of the interaction force. At the same time, for a layer of well-defined thickness (like in our case) we do not expect significant variations of  $\epsilon$  unless the layer is non-stoichiometric. In the latter case, local changes of composition can cause considerable variations of dielectric properties. On the other hand, significant influence on the surface potential distribution can be expected from intrinsic or dipole charges. Dipoles consisting of mobile electrons and unscreened immobile dopant atoms can be formed in the ultra-thin LAO layer in a similar way as it has been found for semiconductors.<sup>19</sup> However, to properly consider the effect of polarization for the ultra-thin LAO layers with the conductive interface beneath, one should also take into account the role of this interface as a kind of electrical shield separating the top LAO layer from the STO substrate.

### 3. RESULTS AND DISCUSSION

In order to prove the applicability of KPFM to planar studies of LAO/STO interfaces, a surface of 4  $\mu\text{m}$  thick layer was lithographically masked and  $3 \times 3 \mu\text{m}$  squares were irradiated by 250 eV Ar<sup>+</sup> ions. After that the photoresist mask was removed. AFM and KPFM images of one of these squares are presented in Figure 1. The AFM image shows a smooth LAO surface with terraces originating from atomic steps of the slightly miscut STO surface. The KPFM image does not reproduce topography, but rather demonstrates a clear difference in surface potential between the unirradiated and irradiated areas. The unirradiated area has much lower potential. It can be interpreted as a lower charge density due to suppressed dipole formation caused by the presence of the conductive interface which electrically shields the LAO layer from the STO. On the other hand, the LAO layer inside the irradiated area is amorphized and the conductive interface is destroyed (the squares become insulating). The numerous structural defects (especially vacancies) give rise to charge carriers favouring a dipole formation under the bias applied between tip and surface. This explains much higher values of the surface potential inside the irradiated squares.

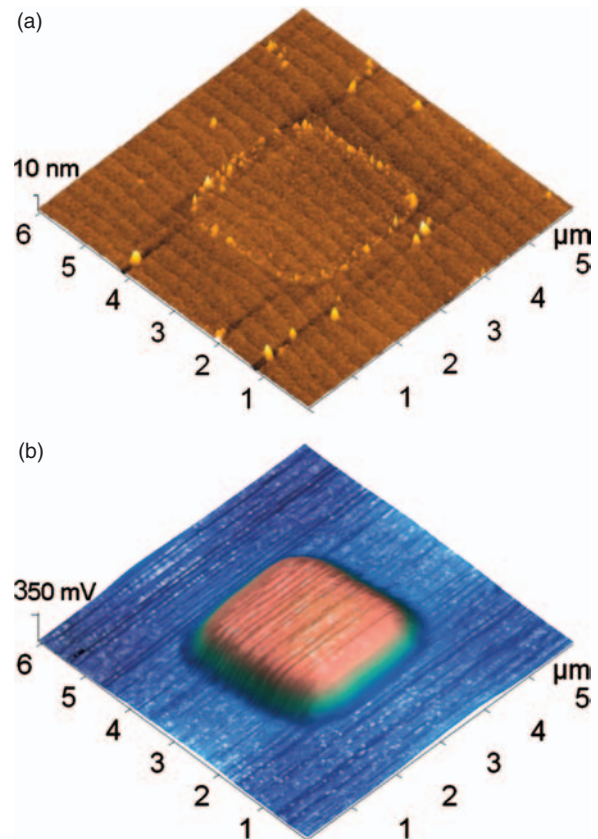


**Fig. 1.** (a) AFM and (b) KPFM images of LAO/STO sample with 4  $\mu\text{m}$  thick LAO layer. The LAO layer is radiation-damaged and conductivity of the interface is destroyed inside the centrally positioned square. The small bumps at the square perimeter in (a) correspond to residual photoresist.



Now we switch to the as-grown and annealed samples (i.e., without radiation damage). Typical surface potential image from bare STO substrate is presented in Figure 2(a). The scale on the right-hand side shows the relative variation of the potential with respect to a mean value. The STO substrate demonstrates rather homogeneous distribution of the surface potential that indicates absence of significant variations of the dielectric properties and surface charges. The image in Figure 2(b) corresponds to 2  $\mu\text{c}$  thick LAO layer deposited on the STO. This image is a typical one, i.e., similar surface potential distributions were observed on other samples with 2  $\mu\text{c}$  thick LAO layer. Moreover, samples with 3  $\mu\text{c}$  thick layer demonstrate same type of the island-like potential images and therefore not shown. Pronounced island-like structure presented in Figure 2(b) is rather different from that found for bare STO. This type of island-like structure is observed in considerable number of scans over the same area, thus, eliminating possible contribution of surface contaminants. The surface potential of 4  $\mu\text{c}$  thick layer changes back to an almost homogeneous

(or slightly mosaic-like) distribution, see Figure 2(c). Further increase of thickness up to 6  $\mu\text{c}$  leads to a homogeneous potential distribution (Fig. 2(d)), very similar to that observed on bare STO.

The island-like type of surface potential distribution found for 2 and 3  $\mu\text{c}$  thick layers can be related to the formation of areas rich in mobile charge carriers at the LAO/STO interface, thus affecting local polarization of the ultra-thin LAO layers. Formation of these areas may be caused by a local change of composition. This is supported by MEIS results indicating non-stoichiometry in thin ( $\leq 3$   $\mu\text{c}$ ) LAO layers.<sup>9</sup> In particular, deficiency of La was found in the layers and La diffusion into STO was suggested. Substitution of Sr by La is one possible source for increased concentration of charge carriers at the interface. We do not also exclude that charge carriers originate from oxygen-vacancies in the STO.<sup>6,7</sup> It should be emphasised that the areas with increased concentration of mobile charge carriers in 2 and 3  $\mu\text{c}$  thick films do not provide a continuous (or quasi-continuous) conductive path.

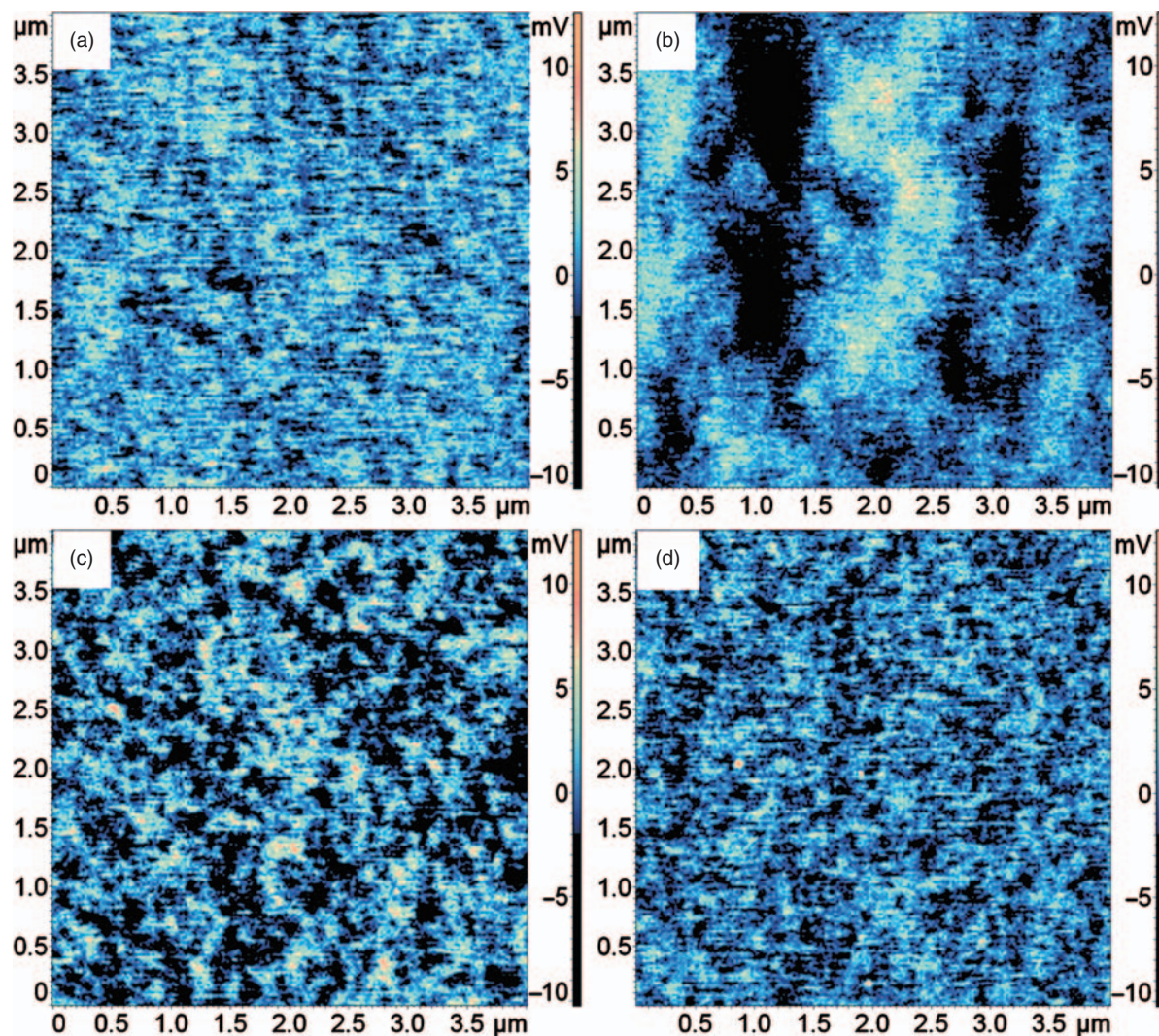
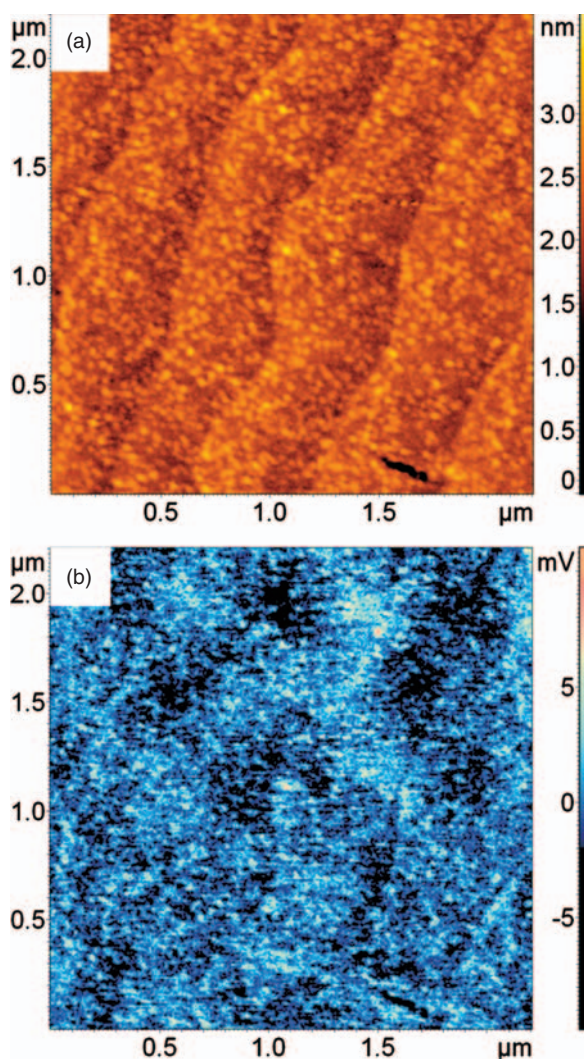


Fig. 2. KPFM images of (a) bare STO substrate and LAO/STO samples with (b) 2, (c) 4 and (d) 6  $\mu\text{c}$  thick LAO layer.



The change from island-like to almost homogeneous potential distribution with increase of the layer thickness from 3 to 4  $\mu\text{c}$  can be interpreted in terms of a change of surface composition towards a stoichiometric one, which is observed using MEIS.<sup>9</sup> The stoichiometry excludes considerable local variations of composition and consequently dielectric properties at surface thus eliminating inhomogeneity in the surface potential distribution. One should also consider the formation of a conductive interface between two dielectrics which acts as an electrical shield separating the LAO layer from the STO substrate. This prevents possible local contributions of charges from the STO substrate on the potential measured at the LAO surface. Thus, the samples with 4  $\mu\text{c}$  thick layer represent a boundary case of insulator-to-metal transition in conductance. This transition is evidenced by KPFM as a change of the surface potential distribution from island-like towards a homogeneous one. The potential distribution becomes even more homogeneous for the samples with

6  $\mu\text{c}$  thick LAO layers due to an enhancement of both mentioned effects (homogeneity in composition and shielding). The presence of a shielding effect can even be quantified. It is found that the absolute values of the surface potential in the case of 4 and 6  $\mu\text{c}$  thick layers are, on average, about 2 times lower than those measured for 2 and 3  $\mu\text{c}$  thick ones. It means that the presence of conductive interface beneath the layers leads to less efficient polarization, i.e., to much lower surface potential, and prevents contributions from the STO substrate that could cause an inhomogeneity in the surface potential distribution. For rather thick (10  $\mu\text{c}$ ) LAO layers, the contribution of topography becomes visible in the KPFM images (Figs. 3(a and b)). Possible origins can be related to both an enhanced dipole formation at the atomic steps in rather thick layers and almost no shielding because the conductive interface is well below the surface. It is probably too deep to effect on the electrostatic properties of the top surface layers.



**Fig. 3.** (a) AFM and (b) KPFM images of 10  $\mu\text{c}$  thick LAO layer deposited on STO.

#### 4. CONCLUSIONS

The dependencies of surface potential on thickness of the LAO layers deposited on STO substrates are studied. These data are compared with previously obtained results on the change of composition of the LAO/STO heterointerfaces with increasing LAO thickness. KPFM shows an evolution in the planar distribution of the surface potential from an island-like to a homogeneous one. It is suggested that the islands observed for 2 and 3  $\mu\text{c}$  thick layers correspond to areas with enhanced concentration of charge carriers at the interface due to local variations of the composition mainly related to the La interdiffusion. Increasing the thickness up to 4  $\mu\text{c}$ , islands rich of charge carriers grow and the interface becomes conductive. Thus, the KPFM results support a percolation model<sup>9</sup> to explain the insulator-to-metal transition in LAO/STO.

**Acknowledgments:** We acknowledge the financial support from EU FP6 “Nanoxide,” VR grant “Oxidelektronik” and KAW foundation. We are also grateful to Professor Øyesten Fischer for valuable discussions.

#### References and Notes

1. A. Ohtomo and H. Y. Hwang, *Nature* 427, 423 (2004); 441, 120 (2006).
2. A. D. Caviglia, S. Gariglio, N. Reyren, D. Jaccard, T. Schneider, M. Gabay, S. Thiel, G. Hammerl, J. Mannhart, and J.-M. Triscone, *Nature* 456, 624 (2008).
3. S. Thiel, G. Hammerl, A. Schmehl, C. W. Schneider, and J. Mannhart, *Science* 313, 1942 (2006).
4. A. Brinkman, M. Huijben, M. Van Zalk, J. Huijben, U. Zeitler, J. C. Maan, W. G. Van Der Wiel, G. Rijnders, D. H. A. Blank, and H. Hilgenkamp, *Nature Mater.* 6, 493 (2007).
5. N. Nakagawa, H. Y. Hwang, and D. A. Muller, *Nature Mater.* 5, 204 (2006).

6. W. Siemons, G. Koster, H. Yamamoto, W. A. Harrison, G. Lukovsky, T. H. Geballe, D. H. A. Blank, and M. R. Beasley, *Phys. Rev. Lett.* 98, 196802 (2007).
7. A. Kalabukhov, R. Gunnarsson, J. Börjesson, E. Olsson, T. Claeson, and D. Winkler, *Phys. Rev. B* 75, 121404(R) (2007).
8. P. R. Willmott, S. A. Pauli, R. Herger, C. M. Schlepütz, D. Kumah, C. Cionca, and Y. Yacoby, *Phys. Rev. Lett.* 99, 155502 (2007).
9. A. Kalabukhov, Yu. A. Boikov, I. T. Serenkov, V. I. Sakharov, V. N. Popok, R. Gunnarsson, J. Börjesson, N. Ljustina, E. Olsson, D. Winkler, and T. Claeson, *Phys. Rev. Lett.* 103, 146101 (2009).
10. C. L. Jia, S. B. Mi, M. Faley, U. Poppe, J. Schubert, and K. Urban, *Phys. Rev. B* 79, 081405(R) (2009).
11. J. Börjesson, PhD Thesis, Chalmers University of Technology, Gothenburg (2009).
12. M. Nonnenmacher, M. O'Boyle, and H. K. Wickramasinghe, *Appl. Phys. Lett.* 58, 2921 (1991).
13. Y. Rosenwaks, R. Shikler, Th. Glatzel, and S. Sadewasser, *Phys. Rev. B* 70, 085320 (2004).
14. H. Huang, H. Wang, J. Zhang, and D. Yan, *Appl. Phys. A* 95, 125 (2009).
15. J. D. Jackson, *Classical Electrodynamics*, Wiley, New York (1998).
16. S. Kalinin and D. A. Bonnell, *Phys. Rev. B* 62, 10419 (2000).
17. Y. Shen, D. M. Barnett, and P. M. Pinsky, *Rev. Sci. Instrum.* 79, 023711 (2008).
18. L. Yan, *Semicond. Sci. Technol.* 19, 935 (2004).
19. C. Baumgart, M. Helm, and H. Schmidt, *Phys. Rev. B* 80, 085305 (2009).

Received: 24 March 2010. Accepted: 26 April 2010.